Efficient 50S Ribosome-Catalyzed Peptide Bond Synthesis with an Aminoacyl Minihelix†

Niranjan Y. Sardesai,‡ Rachel Green,§ and Paul Schimmel*,‡

The Skaggs Institute for Chemical Biology, The Scripps Research Institute,10550 North Torrey Pines Road, La Jolla, California 92037, and Department of Molecular Biology and Genetics, Johns Hopkins University, School of Medicine, Baltimore, Maryland 21205

Received May 17, 1999

ABSTRACT: RNA minihelices that recreate the amino acid acceptor domain of the two-domain L-shaped tRNA molecule are substrates for specific aminoacylation by tRNA synthetases. Some lines of evidence suggest that this domain arose independently of and predated the second, anticodon-containing domain. With puromycin and a minihelix charged with alanine, we show here efficient 50S ribosome catalyzed peptide synthesis. The aminoacyl minihelix is as active as aminoacyl tRNA in the synthetic reaction. The high efficiency of the charged minihelix is due to a relatively strong interaction with the 50S particle. In contrast, an aminoacyl RNA fragment that recreates the 3′-side of the tRNA acceptor stem has a much weaker interaction with the 50S particle. These results are consistent with the minihelix domain being the major loci for tRNA interactions with the 50S ribosome. They may also have implications for the historical development of RNA-based systems of peptide synthesis.

Ribosomes play a central role in biological protein synthesis. Although differences exist in the mechanistic details of translation among prokaryotes and eukaryotes, the basic architecture and peptidyl transfer reaction catalyzed by the ribosome is conserved in all three branches of the tree of life. The ribosome consists of 2 subunits (large and small) and, in *E. coli* (70S ribosome), comprises about 55 proteins and 3 RNAs: 5S (120 nt), 16S (1542 nt), and 23S (2904 nt). Both RNA and protein components of the ribosome have conserved sequences and secondary structures (*1*−*3*) across the three taxonomic domains, suggesting that ribosome origins may have predated the separation of life into three branches (*4*). Elucidating a mechanism for the assembly of the ribosome in evolution can provide insights into the origin of protein synthesis.

Early work demonstrated that the ribosomal proteins and RNAs were segregated into a large (50S) and a small (30S) subunit. The two subunits can each be reconstituted from their components (*5*−*9*), consistent with the possibility that they arose separately. The possible independent development of two ribosome subunits was further supported by the observation that they have distinct functions. The 50S subunit contains 23S and 5S rRNA and is the site of catalysis (peptidyl transfer). The 30S subunit (containing 16S rRNA) is the seat of the codon−anticodon interaction (decoding site). Significantly, under certain conditions, peptidyl transfer and decoding functions can be uncoupled; that is, the 50S subunit can catalyze peptidyl transfer reactions and polypeptide synthesis in a template-independent manner (*10*). Because the early polypeptides could have been synthesized in the absence of a template, the 50S subunit may have preceded the 30S subunit in evolution.

The tRNAs are carriers for amino acids to the ribosome. The specific aminoacylation of tRNAs establishes the genetic code by linking an amino acid with a specific nucleotide triplet (anticodon) (*11*, *12*). The tRNAs are L-shaped with each arm of the L constituting a separate domain. One arm—the acceptor stem−TΨC minihelix—contains the universal 3′-CCA end with the amino acid attachment site (Figure 1). The other arm contains the anticodon triplet that pairs with the complementary trinucleotide codon on the mRNA. In a number of systems, the two domains of tRNAs exhibit segregated functions. For example, the acceptor stem−TΨC minihelix domain in isolation is a substrate for specific aminoacylation by at least 10 aminoacyl tRNA synthetases (aaRSs)[1] (*13*−*19*), for CCA addition by nucleotidyl transferase (*20*), for binding by elongation factor-Tu (*21*−*23*), and for 5′-processing by RNase P (*24*). Significantly, the two domains of tRNA interact with separate domains of the 70S ribosome (*25*). In particular, the anticodon-containing domain of tRNA interacts with the 30S particle (*26*−*28*) while the minihelix domain interacts with the 50S subunit (*29*, *30*).

These observations raise the possibility that the minihelix domain of tRNAs and the 50S ribosome subunit are progenitors of the full tRNA and 70S ribosome, respectively.

† Supported by Grant GM15539 from the National Institutes of Health. N.Y.S. thanks The Skaggs Institute for Chemical Biology for fellowship support.

* To whom correspondence should be addressed. Fax: (619) 784-8990. E-mail: schimmel@scripps.edu.

‡ The Scripps Research Institute.

§ Johns Hopkins University.

[1] Abbreviations: aaRS, aminoacyl tRNA synthetase; AlaRS, alanine tRNA synthetase; HEPES, *N*-(2-hydroxyethyl)piperazine-*N*′-2-ethanesulfonic acid; Tris, tris(hydroxymethyl)aminomethane; RNase T1, ribonuclease T1; Ac, acetyl; NAP, *N*-acetylalanyl-puromycin; NMP, *N*-acetylmethionyl-puromycin; AcAla-RNA, *N*-acetylaminoacyl-RNA; TLC, thin-layer chromatography.

10.1021/bi991126f CCC: $18.00
Published on Web 08/24/1999

With this in mind, we investigated whether the acceptor stem−TΨC minihelix domain alone can function as an efficient aminoacyl (or peptidyl) carrier in peptide synthesis by the 50S ribosome. We were particularly interested to determine the relative efficiency of peptide synthesis with an aminoacyl minihelix as compared with aminoacyl tRNA. A robust peptide synthesis with 50S ribosomes and charged minihelix substrates would further support the concept of a modular assembly of the contemporary peptide synthesis apparatus.

The 50S particle has two sites that engage acylated tRNAs; the A site binds aminoacyl tRNAs, and the P site binds peptidyl tRNAs (for a review on substrate specificity, see ref *31*). The antibiotic puromycin binds to the A site and has proved to be particularly useful to delineate requirements for P-site substrates. Indeed, Monro et al. first showed a requirement for N-acetylation or N-formylation of the P site aminoacyl RNA substrate for peptide synthesis with puromycin (*32*, *33*). The puromycin reaction was shown to occur with the 50S particle alone with charged tRNA or oligonucleotide substrates bearing the universal CCA-3′ trinucleotide common to all tRNAs (*34*). Thus, this reaction offered the opportunity to investigate a minihelix substrate for peptide synthesis, to determine whether it had all of the tRNA determinants for peptide synthesis that were encoded by the full tRNA.

MATERIALS AND METHODS

Reagents and Enzymes. All reagents, salts, and buffers were purchased from Sigma Chemical Co. (St. Louis, MO) unless indicated otherwise. Radiolabeled [^{3}H]- and [^{14}C]-L-alanine were purchased from Amersham Life Science (Arlington Heights, IL), and [γ-^{32}P]ATP was obtained from NEN Life Science Products (Boston, MA). Polynucleotide kinase (T4) was from New England Biolabs (Beverly, MA) and sequence-grade RNase T1 from Amersham−Pharmacia Biotech (Piscataway, NJ). The 461-residue N-terminal fragment (461N) of *E. coli* AlaRS was overexpressed as a 6-His-tagged protein from plasmid pQE-*alaS*-459-6H in *E. coli* strain TG1 and purified by Ni−NTA (Qiagen, Chatsworth, CA) affinity chromatography as described previously (*35*).

RNA Substrates. Minihelix^{Ala} (35 nt) was synthesized on a Pharmacia synthesizer (Model Gene Assembler Special) using *N*-phenoxyacetyl-protected 2′-*tert*-butyldimethylsilyl-ribonucleoside 3′-cyanoethyl phosphoramidites from Chem Genes (Waltham, MA). The RNA was deprotected using the method of Wincott et al. (*36*) and purified to homogeneity by electrophoresis on a 14% polyacrylamide−8 M urea gel. *E. coli* tRNA^{Ala} was a kind gift of Dr. Magali Frugier.

E. coli 50S ribosome particles were prepared as reported by Moazed and Noller (*37*).

N-Acetylalanyl-RNA Synthesis. Aminoacylation reactions were carried out at room temperature in a reaction mixture (100 μL final volume) containing minihelix^{Ala} or tRNA^{Ala} (1000 pmol), 50 mM HEPES buffer (pH 7.5), 10 mM $MgCl_2$, 20 mM KCl, 20 mM β-mercaptoethanol, 3.2 mM ATP, 12.5 μM [^{3}H]-L-alanine, 50 μM L-alanine, and 1.0 μM 461N fragment of *E. coli* AlaRS. After allowing the reaction to proceed for 60 min, the mixture was extracted twice with phenol [saturated with citrate buffer (pH 4.5)]−chloroform (1:1) to remove the enzyme component. The organic layer was back-extracted with water (100 μL), and the aminoacyl-RNA product in the combined aqueous volume was recovered by ethanol precipitation. All ethanol precipitation steps (here and below) were carried out using 3.0 M sodium acetate (pH 5.2), to minimize hydrolysis of the aminoacyl ester linkage. The Ala-RNA^{Ala} pellet was rinsed with chilled 80% ethanol and dried on a rotary evaporator. About 70−80% of the RNA is aminoacylated under these conditions, based on the specific activity of the [^{3}H]-L-alanine incorporated.

The Ala-RNA^{Ala} pellet was resuspended in 100 μL of sodium acetate (0.2 M, pH 6.0) and reacted on ice with 2 × 50 μL aliquots of acetic anhydride [Fluka (Buchs, Switzerland)] for 40 min following the protocol of Haenni and Chapeville (*38*). The *N*-acetylalanyl-RNA (AcAla-RNA) product was recovered by ethanol precipitation followed by a chilled 80% EtOH rinse. The AcAla-RNA was stored dry at −20 °C in 100 pmol aliquots until further use.

Synthesis of AcAla-9mer. AcAla-minihelix^{Ala} (20−100 pmol) was treated with RNase T1 (0.5−1.0 unit) in 15 mM sodium acetate (pH 5.2), 1 mM EDTA, at room temperature for 30 min and then placed on ice.

Peptidyl Transfer Assay. Aliquots of AcAla-RNA were resuspended in a 10 μL volume of resuspension buffer [15 mM sodium acetate (pH 5.2), 1 mM EDTA] and stored on ice. The specific activity of the [^{3}H]-L-alanine used in the aminoacylation reaction was used to determine the concentration of AcAla-RNA in the stock solution. Reactions were carried out on ice with mixtures containing the following (20−35 μL total volume): ribosomal 50S subunits and AcAla-RNA substrates at the indicated final concentrations; 0.4 M potassium acetate; 50 mM HEPES (pH 8.3); 100 mM $MgCl_2$; 1 mM puromycin (neutralized); and 20% MeOH (by volume). Reactions were initiated by the addition of puromycin dissolved in MeOH immediately after addition of the AcAla-RNA substrate to buffer containing 50S subunits. In parallel, a TLC plate [EM Science (Gibbstown, NJ), 20 cm × 10 cm (Silica Gel 60), 250 μm thick with 250 nm (excitation) fluorescent indicator] was first acidified by prerunning in 1-butanol/acetic acid/water (4:0.9:1) for 2 cm and then allowing the plate to dry. Aliquots (3−5 μL) of the reaction mixture were removed at the indicated time points and quenched by spotting directly on the TLC plate. Next, the TLC plate was developed in 1-butanol/acetic acid/water (4:0.9:1) (*39*, *40*) until the solvent front was about 7 cm from the origin and, then, dried completely before visualization by fluorimagery.

Visualization and Quantitation of Products. The TLC plate was sprayed with EN^{3}HANCE spray (NEN Life Science Products) and visualized by fluorimagery by exposing to an X-ray film at −80 °C for 1−5 days. Band intensities on the film were quantified by using a densitometer [Molecular Dynamics (Sunnyvale, CA)] and analyzed by Image Quant analysis software. Predetermined amounts of [^{3}H]-L-alanine were spotted on the top portion of the TLC plate (above the solvent front) prior to fluorimagery. Calibration curves thus obtained allowed us to determine the optimal exposure times for the X-ray film so as to remain within the linear range of the response of the film and to not saturate the response of the densitometer.

The band intensity of the N-AcAla-puromycin product (NAP) as well as the intensity of the unreacted AcAla-RNA (at the origin O) [(AcAla-RNA)$_O$] was quantified. The

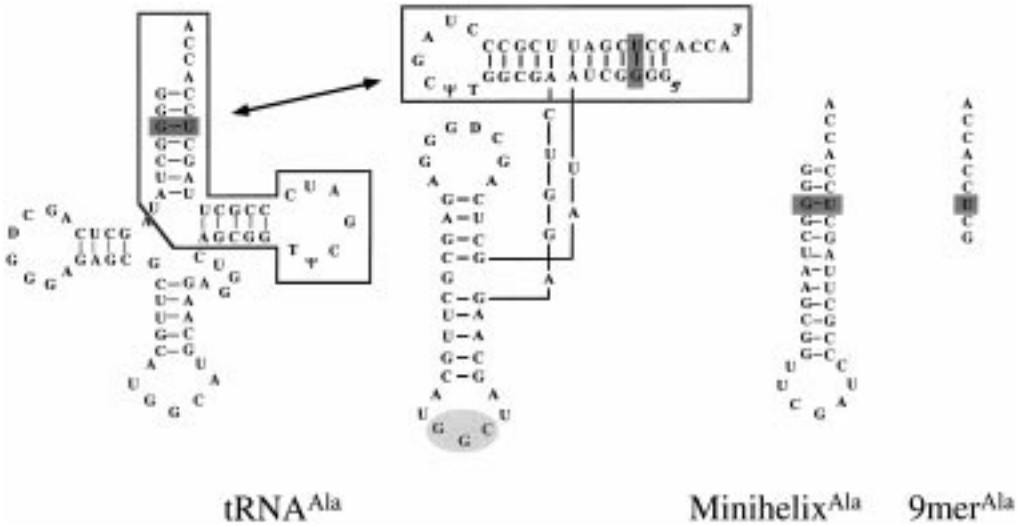

FIGURE 1: RNA substrates used in this study. The secondary structure of *E. coli* tRNA^{Ala} is shown in the cloverleaf form (left) together with the L-shaped arrangement seen in the three-dimensional structure. The minihelix domain with the universal CCA-3′ amino acid acceptor end is boxed in the L-shaped representation. The G3:U70 pair that is essential for aminoacylation of tRNA^{Ala} is enclosed in a shaded rectangle. Anticodon trinucleotides are highlighted in a shaded ellipse. Minihelix^{Ala} was synthesized chemically, and fragment 9mer^{Ala} (far right) was obtained by the digestion of minihelix^{Ala} with RNase T1.

fraction converted was calculated as $f = [(\text{NAP})/((\text{AcAla-RNA})_O + (\text{NAP}))]$. The fraction converted was transformed into picomoles of NAP formed per aliquot as follows: $f \times$ (initial concentration of AcAla-RNA in micromolar) $\times$ (volume per aliquot). Data are plotted as NAP formed (in picomoles) versus time and represent the average of 2−4 independent experiments.

RESULTS

In the experiments described below, our strategy was to prepare activated amino acids in the form of aminoacyl minihelices that could donate the aminoacyl group for peptide synthesis. For comparison, we also prepared the intact aminoacyl tRNA substrate that is used universally for ribosome-dependent protein synthesis. These two formats for presentation of the activated aminoacyl group were then used under conditions where the free amino group of puromycin bound at the ribosomal A site reacts with the activated carbonyl carbon of the aminoacyl group of aminoacyl RNA (minihelix or tRNA). Aware that a single-stranded RNA fragment bearing an aminoacyl group at its 3′-end could also react with ribosome-bound puromycin, we prepared a single-stranded aminoacyl nonamer based on the 3′-side of the minihelix. The question was whether peptide synthesis with the aminoacyl minihelix could be achieved under conditions where peptide bond formation with the charged single-stranded RNA was virtually eliminated.

With puromycin bound at the A site, we directed the charged RNA substrates to the P site by reacting the free amino groups of the aminoacyl-RNAs with acetic anhydride (*N*-acetyl aminoacyl RNAs). With the amino group blocked, the ester linkage is more stable to hydrolysis, and this enhanced stability enabled us to do manipulations with these substrates more freely.

Aminoacylation of Minihelix^{Ala} and tRNA^{Ala}. RNA minihelices that recapitulate the acceptor stem of tRNA^{Ala} are efficient substrates for enzymatic aminoacylation by AlaRS (Figure 1) (*13, 41*). This circumstance allowed us to synthesize in good yield aminoacylated minihelix substrates. Previous studies had shown that an N-terminal 461 residue fragment (461N) aminoacylates tRNA^{Ala} with the same efficiency as it charges minihelix^{Ala} (*42*). Therefore, we carried out the aminoacylation reactions for both tRNA^{Ala} and minihelix^{Ala} using 461N protein so as to minimize differences in alanine incorporation between substrates and to obtain the same specific activity for the charged RNA. Indeed, we calculated that both substrates were charged to an extent of 75−80%. After aminoacylation, the aminoacyl RNAs were reacted with acetic anhydride to yield AcAla-RNA^{Ala}.

In Situ Synthesis of AcAla-9mer Substrate. The AcAla-9mer^{Ala} single-stranded fragment shown in Figure 1 was generated by treating AcAla-minihelix^{Ala} with RNase T1. In preliminary experiments using 5′-^{32}P-end-labeled minihelix^{Ala}, we determined that 0.5 unit of RNase T1 was sufficient to digest completely 20−100 pmol of RNA in 30 min (room temperature) as judged by the disappearance of the 35 nt minihelix substrate (and appearance of a 1 nt product corresponding to 5′-[^{32}P]GMP) following denaturing polyacrylamide gel electrophoresis. Significantly, the acetylaminoacyl ester linkage at the 3′-end of substrate RNA is stable to hydrolysis under the conditions of the RNase T1 digestion. When 3′-([^{14}C]AcAla)-minihelix^{Ala} was used as a substrate under identical digestion conditions for RNase T1, we saw quantitative conversion to the expected 3′-([^{14}C]AcAla)-9mer^{Ala} product as judged by electrophoresis on 20% polyacrylamide−8 M urea−acid gels (pH 5.2) (data not shown).

TLC Assay To Detect Peptidyl Transferase Activity in the "Fragment Reaction". The "fragment reaction" (*33*) has been much used to follow formation of a single peptide bond using model tRNA substrates. The assay follows the nucleophilic attack of puromycin (acting as a ribosomal A-site aminoacyl tRNA analogue) on an *N*-acetylaminoacyl-tRNA analogue (bound to the P-site) to yield an *N*-acetylaminoacyl-puromycin product (in this case, N-AcAla-puromycin or NAP) (Figure 2). While the assay uncouples peptidyl transfer from template dependence, methanol (33 vol %) is a stringent

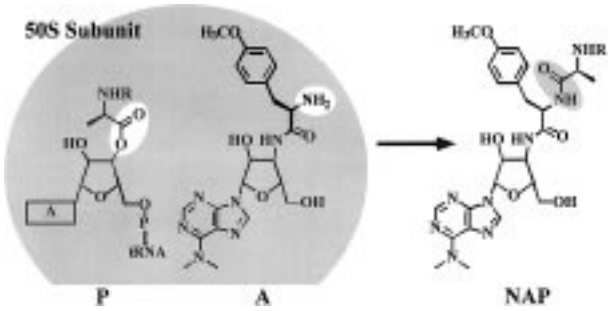

FIGURE 2: Schematic of the puromycin reaction showing the formation of *N*-acetylalanyl-puromycin (R = CH_3CO-) following a single peptidyl transfer event. The amino group and activated carboxylate participating in the condensation reaction are highlighted as is the amide bond that is formed. The radiolabeled amino acid is transferred from the substrate RNA to puromycin. The NAP product is easily resolved by TLC.

requirement to facilitate substrate binding to the P site on the 50S ribosome (*34*). Frequently, radiolabeled activated methionine was used as the amino acid to react with puromycin. The reaction product N-Ac-[^{35}S]Met-puromycin (NMP) was recovered by extraction with ethyl acetate at pH 5.5, and quantitation was accomplished by scintillation counting. Thus, the assay is dependent on the partitioning of the NMP product into the ethyl acetate layer.

We were concerned that quantitative partioning into the organic layer may not be achieved with alanine (and its less hydrophobic side chain) in the expected product (NAP). Moreover, in addition to the expected hydrolysis product of the aminoacyl RNA that competes with the peptidyl transfer reaction, the presence of alcohol in the reaction leads to products of methanolysis; resolution of the products of methanolysis is desirable. Indeed, even with methionine, the best resolution of products was obtained by base hydrolysis of the methyl esters, by selective extraction by ethyl acetate, and, finally, by paper electrophoresis (*43*).

To deal with these concerns, we developed a TLC assay for the detection of *N*-acetylaminoacyl-puromycin. The TLC plates were developed with butanol/acetic acid/water (*39*, *40*),and the resolved NAP was detected by fluorimagery. We chose [^{3}H]alanine for our assays because of its approximately 350-fold higher specific activity compared to the commercially available [^{14}C]alanine. Unlike [^{14}C]amino acids, the low energy of the β-emission from tritium does not allow the use of phosphorimagery for quantitative analysis. However, the significantly greater specific activity of [^{3}H]alanine makes analysis by fluorimagery convenient.

tRNA^{Ala} as a P-Site Substrate for 50S Ribosome-Dependent Peptidyl Transfer. The time-dependent appearance of a band corresponding to NAP occurred when 0.1 μM AcAla-tRNA^{Ala} was incubated with 0.1 μM 50S ribosomes, saturating puromycin (1 mM), and methanol. Puromycin alone or 50S subunits alone did not produce NAP nor was the product seen in the presence of methanol alone (data not shown and see below). The reaction of puromycin with AcAla-RNA^{Ala} did not proceed without the presence of methanol (data not shown), consistent with early observations of Monro (*32*, *34*) with a number of different aminoacyl-tRNA species.

NAP Synthesis with the AcAla Single-Stranded Fragment. In the early studies of Monro and co-workers, an aminoacyl single-stranded 3′-fragment of three to six nucleotides (ending in CCA-3′OH) was active in the puromycin-dependent peptide synthesis reaction. To further check the validity of our assays and to confirm the early work with a similar but distinct substrate that was unique to this study, we carried out the puromycin reaction with 50S ribosomes (1.0 μM) and the AcAla-nonamer RNase T1 fragment (1.0 μM) from the 3′-end of tRNA^{Ala}. A time-dependent synthesis of NAP was observed over a period of 20 min, thus establishing that the fragment-based reaction with the nonamer at 1 μM was similar to the reaction seen in the early studies with the RNA moiety being only three to six nucleotides (Figure 3).

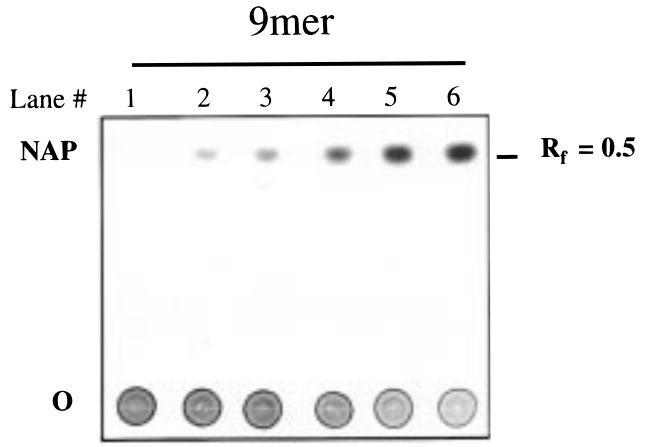

FIGURE 3: Time-dependent formation of NAP using AcAla-9mer^{Ala} as a substrate. Aliquots of the reaction mixture [containing AcAla-9mer^{Ala} (1.0 μM) and 50S particles (1.0 μM)] were spotted on a silica TLC plate at the origin (O) and developed in 1-butanol/acetic acid/water (4:0.9:1). The image is a densitometer scan of an X-ray film exposed to the TLC plate sprayed with EN^{3}HANCE^R fluorimaging reagent. Lanes 1−6 represent 3 μL aliquots removed from the reaction mixture at time t = 1, 3, 5, 10, 15, and 20 min, respectively.

Given the activity of the charged fragment, we imagined that the charged minihelix would also be active in the puromycin reaction. The amount of N-Ac-aminoacyl fragment used in our studies (1 μM) is considerably higher than that needed with N-Ac-aminoacyl-tRNA, where concentrations as low as 0.1 μM were effective (see above and below). The concentration of 50S subunit was also 10-fold higher (1 μM versus 0.1 μM) for the reaction with the fragment than that needed with N-Ac-aminoacyl-tRNA. With this in mind, we were particularly interested to see whether peptide synthesis with Ac-Ala-minihelix^{Ala} could be detected at RNA and 50S ribosome concentrations comparable to those effective with the tRNA substrate, or whether the minihelix would be no different in reactivity than a small single-stranded fragment.

Efficient Peptide Synthesis with AcAla-Minihelix^{Ala}. We first investigated the charged minihelix at a concentration of 0.1 μM with 1.0 μM 50S ribosomes. As shown in Figure 4a, synthesis of NAP was easily detected over a time period of 10 min. The product (R_f = 0.5) is observed only when 50S subunits, puromycin and methanol, are present in the reaction mixture (lanes 9−12). NAP synthesis was not observed in the presence of methanol and 50S subunits (lanes 1−4), methanol and puromycin (lanes 5−8), or methanol alone (lanes 13−16).

Although the control experiments above indicated otherwise, we were concerned that the presence of 50S subunits

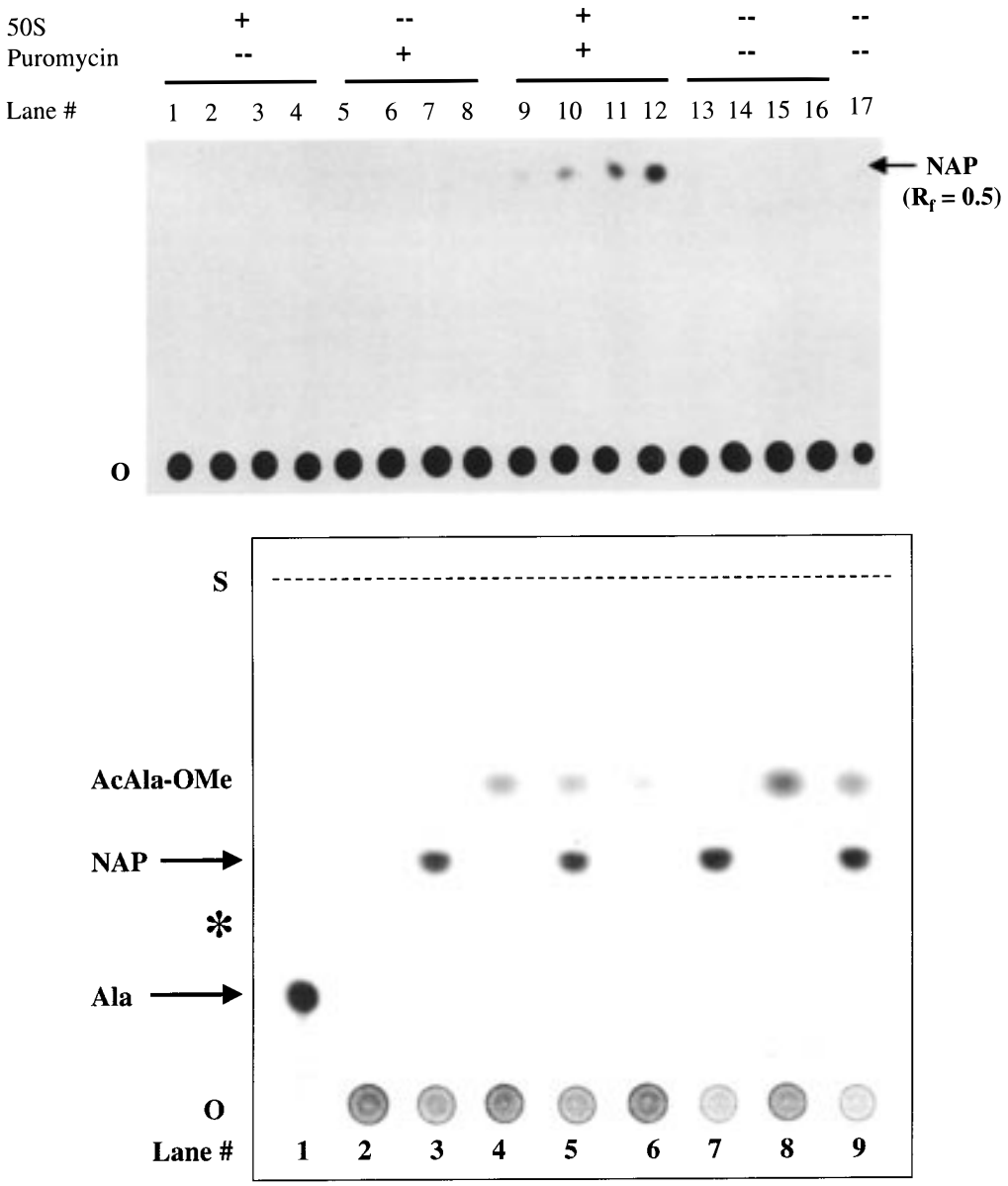

FIGURE 4: (a) Time-dependent formation of NAP with AcAla-minihelix^{Ala} as a substrate together with controls showing the requirement of 50S ribosomes and puromycin. The fluorimage was processed as described in Figure 3. All reactions [AcAla-minihelix^{Ala} (0.1 μM), 50S particles (1.0 μM), and puromycin (1.0 mM)] were carried out in 20% MeOH (vol %). Lanes 1−4, 5−8, 9−12, and 13−16 represent 3 μL aliquots spotted at time t = 1, 3, 5, and 10 min, respectively. Lane 17 shows a control where AcAla-minihelix^{Ala} was spotted after incubation for 30 min in pH 5.2 resuspension buffer. No hydrolysis products were observed, thus showing that the aminoacyl ester linkage is stable during the course of the experiment. (b) Controls showing synthesis of AcAla-OMe and NAP. AcAla-minihelix^{Ala} (1.0 μM) was treated with 20% (vol) MeOH (lanes 2, 4, 6, 8) or MeOH (20% vol), 50S subunits (1.0 μM), and puromycin (1 mM) (lanes 3, 5, 7, 9) and spotted at the origin (O). Lanes 2−5 and 6−9 represent 3 μL aliquots spotted at time t = 20 and 60 min, respectively. Reactions in lanes 2, 3, 6, and 7 were carried out at 4 °C and in lanes 4, 5, 8, and 9 at 24 °C (room temperature). A small amount of [^{3}H]Ala was spotted in lane 1. Also shown is the position of AcAla (*) standard, solvent front (S).

and puromycin may stimulate formation of methanolysis (AcAla-OMe) or hydrolysis (AcAla-OH) products of AcAla-RNA^{Ala} that would incorrectly contribute to the rates of NAP synthesis if they comigrated with the desired product (*44*). Therefore, identification and resolution of these side products was critical to our experiment. Indeed, when we exposed the X-ray film for an extended period of time (so that the NAP and AcAla-RNA^{Ala} bands were over-exposed), a small amount of a second product (R_f = 0.65) migrating faster than NAP was observed (data not shown and see below).

Next, we ascertained that the faster migrating product was AcAla-OMe and determined conditions under which its production was minimized (Figure 4b). We treated 1.0 μM AcAla-minihelix^{Ala} with methanol alone (20 vol %) or with methanol, 50S subunits (1.0 μM), and puromycin (1 mM) at 4 °C (on ice) or at 24 °C (room temperature) and assayed aliquots of the reaction mixture at 20 and 60 min. As expected, substantial NAP synthesis (R_f = 0.5) was observed at both temperatures (lanes 3, 5, 7, and 9) and was absent in the lanes containing methanol alone (lanes 2, 4, 6, and 8). In addition, we observed production of a faster migrating second band at 24 °C (lanes 4, 5, 8, and 9) within 20 min. Because this product was observed even in the absence of 50S subunits and puromycin, but not in the absence of methanol [data from Figure 4a (lane 17) and data not shown], we identify it as AcAla-OMe (R_f = 0.65). Importantly, at 4

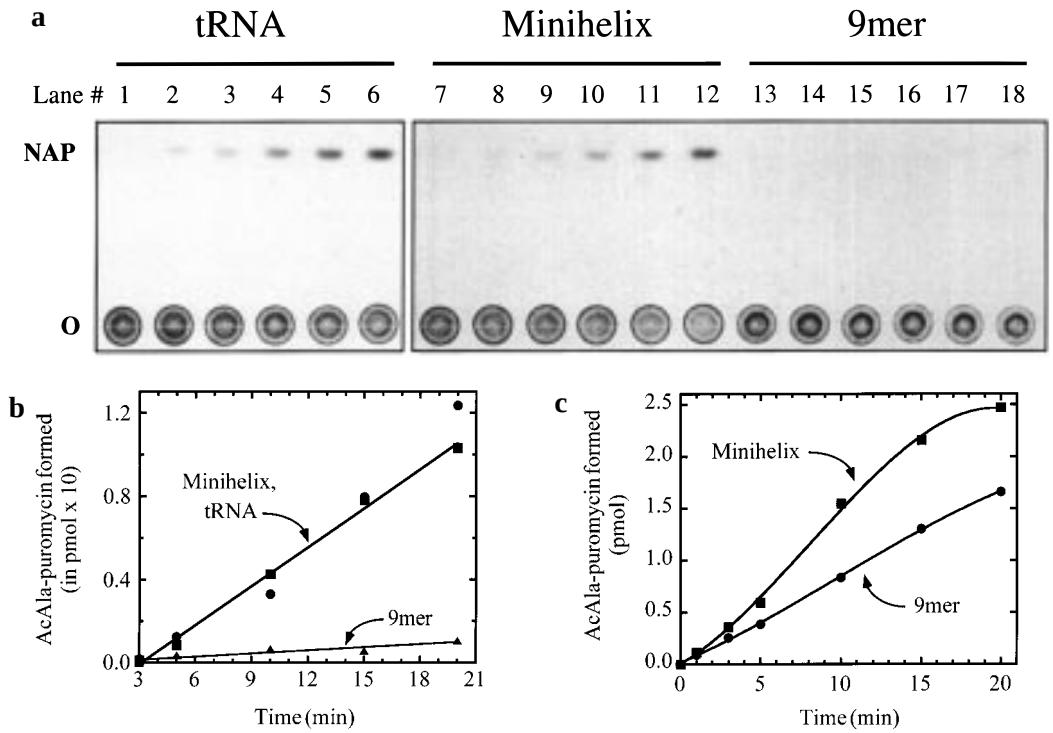

FIGURE 5: (a) Fluorimage (processed as in Figure 3) comparing rates of NAP synthesis using tRNA^{Ala} (lanes 1−6), minihelix^{Ala} (lanes 7−12), and 9mer^{Ala} (lanes 13−18) as substrates. Lanes 1−6, 7−12, and 13−18 represent 5 μL aliquots removed from the reaction mixture [AcAla-RNA^{Ala} (0.1 μM) and 50S particles (0.1 μM)] at time t = 1, 3, 5, 10, 15, and 20 min, respectively. (b) Band intensity of NAP product formed in part a quantified and expressed in picomoles of NAP formed versus time [starting at time t = 3 min because of the low concentration of 50S ribosome (see text)]. (c) Comparison of NAP synthesis when 10-fold higher concentrations of AcAla-minihelix^{Ala} or AcAla-9mer^{Ala} and of 50S ribosome are used (1.0 μM of each). The rate of NAP synthesis stated in the text was calculated from the slope of the linear part of the curve (3−10 min).

°C we observed only a small amount of AcAla-OMe formed at 60 min (lanes 6 and 7) and an insignificant amount at 20 min (observed only when the film was over-exposed) (lanes 2 and 3 and data not shown). With the charged minihelix, we estimate that the amount of AcAla-OMe produced as a side product in 20 min at 4 °C is at least 100-fold less than the amount of NAP produced under the same conditions.

When we used Tris−KOAc (pH 8.3) in place of HEPES−KOAc (pH 8.3) in our controls lacking 50S ribosome, we observed greater amounts of methanolysis and hydrolysis at both temperatures (data not shown). Therefore, we carried out quantitative assays in HEPES−KOAc buffer at 4 °C. In parallel, using ^{3}H-labeled standards, we determined that Ala migrated with an R_f = 0.25 (Figure 4b, lane 1) and AcAla-OH with an R_f = 0.4 under the conditions of our TLC assay. Thus, the AcAla-RNA^{Ala} substrate and all of the ^{3}H-labeled products in the reaction are well resolved from NAP and from one another.

In Contrast to AcAla-9mer^{Ala}, AcAla-tRNA^{Ala} and AcAla-Minihelix^{Ala} Are Equally Efficient Substrates for Peptidyl Transfer. We lowered the concentration of ribosome to 0.1 μM to match that of AcAla-minihelix^{Ala}. Synthesis of NAP was still detected at these reduced concentrations. At low ribosome concentrations, we observed an initial slow phase (approximately 3 min, data not shown) after which the rate of NAP synthesis was linear with time. This time period likely corresponds to equilibration of the ribosome P-site with AcAla-RNA^{Ala} and is consistent with the use of short preincubation times (approximately 5 min) in the puromycin reactions (*43*). A stimulation of rates also has been observed following a short preincubation at higher temperatures (40 °C) (*45*), suggesting a rearrangement of ribosome structure to a more active conformation. Therefore, at low ribosome concentration we measured the rates starting at 3 min after initiation of the reaction.

We then investigated whether the AcAla-9mer^{Ala} single-stranded fragment at a concentration of 0.1 μM with 0.1 μM 50S ribosome was deficient as a substrate in the peptide synthesis reaction with puromycin (see below). Using these concentrations, AcAla-tRNA^{Ala}, AcAla-minihelix^{Ala}, and the AcAla-9mer^{Ala} fragment were compared side-by-side. With AcAla-minihelix^{Ala}, an efficient synthesis of NAP occurred with approximately 30% of the reaction being completed within 20 min (Figure 5a,b) with an observed rate of 1.25 $\times$ 10^{-9} M min^{-1}. The apparent bimolecular rate constant was calculated as 2100 M^{-1} s^{-1}.

When the concentration of charged minihelix was reduced by half, the rate of peptide synthesis also decreased by approximately 50% to 0.65 $\times$ 10^{-9} M min^{-1} (data not shown). With AcAla-tRNA^{Ala} in place of the minihelix substrate, a rate of NAP synthesis similar to that observed with the minihelix was seen (Figure 5a,b). The same 50% decrease in rate also was observed when the AcAla-tRNA^{Ala} concentration was decreased to 0.05 μM (data not shown).

In contrast, at these concentrations of RNA substrate and 50S particle, little NAP synthesis could be detected with AcAla-9mer^{Ala} even at 20 min (Figure 5a,b). Because longer exposure of the film resulted in saturating the intensity of the band at the origin (unreacted AcAla-9mer^{Ala}), we could not accurately determine the rate of synthesis with this substrate at a concentration of 0.1 μM. Although we could not see products visually (Figure 5a, lanes 13−18), we

estimated an upper limit for the observed reaction rate of 0.1×10^{-9} M min^{-1} (and apparent bimolecular rate constant of 167 M^{-1} s^{-1}) by densitometric analysis of the film at predicted locations of the NAP product. Thus, with a quantitative comparison, all of the information in tRNA needed for efficient peptide synthesis was seen to be contained in the minihelix domain (Figure 5b). In contrast, the single-stranded 3′-side of the minihelix lacks important RNA structural determinants for peptide synthesis.

Because the AcAla-9mer^{Ala} substrate was generated in situ by the action of RNase T1 just prior to the addition of the 50S particle and puromycin, the RNase T1 which was carried over to the peptide synthesis reaction could in principle inhibit the peptidyl transfer activity of the ribosome. We were particularly concerned about the integrity of the P loop known to be critical for binding C74 of the peptidyl tRNA substrate (*30*). Thus, it was possible that the results from the *in situ* generated AcAla-9mer^{Ala} underestimated the actual efficiency of synthesis. To address this concern, we carried out experiments with AcAla-minihelix^{Ala} where RNase T1 (0.5 unit) was added simultaneously with 50S ribosomes and puromycin. (This amount of RNase T1 was sufficient to generate quantitatively the AcAla-9mer^{Ala} from the precursor charged minihelix.) The presence of 0.5 unit of RNase T1 in the reaction did not reduce the peptidyl transfer reaction (data not shown) with the AcAla-minihelix^{Ala} substrate. The lack of an apparent effect of RNase T1 on the 50S subunits is probably because our assays were carried out at 4 °C and in the presence of 20% methanol; these conditions are known to suppress nuclease activity (*46*). As a further control, we digested unmodified minihelix^{Ala} with RNase T1 (0.5 unit) and added the digestion mix (at 0.1 μM final concentration) to a reaction mixture containing AcAla-minihelix^{Ala} (at 0.1 or 0.05 μM), 50S ribosome, and puromycin. We saw no effect of the digested RNA minihelix on the peptidyl transfer rate of AcAla-minihelix^{Ala} (data not shown). This control established that the other (smaller) 1−5 nt RNase T1 digestion products of minihelix^{Ala} do not interfere with the peptidyl transfer reaction (e.g., by competitive inhibition). Finally, we isolated the RNase T1 digested AcAla-9mer^{Ala} by paper electrophoresis and independently confirmed that the purified fragment was deficient for peptidyl transfer at the lower concentrations (data not shown).

Thus, the difference in the efficiency of peptidyl transfer between AcAla-minihelix and the charged 9-mer is intrinsic to differences in the RNA structures. Because the rates of NAP formation using tRNA or minihelix are similar to each other under conditions when the 9-mer "fragment" is no longer an effective substrate, the minihelix domain of tRNA must contain the predominant functional binding interactions with the 50S subunit.

Maximum Rate of Peptide Synthesis Is Nearly Independent of the RNA Substrate. The puromycin reaction is particularly useful because one of the components (puromycin) of the ternary system can be provided at saturating concentration and because the puromycin substrate is effectively specific for the ribosomal A site. At a 1 mM concentration of puromycin, the A site is completely occupied, and the reaction rate is dependent only on the concentration of the P-site substrate (*47, 48*). Indeed, when NAP synthesis is carried out using relatively high concentrations of 50S ribosomes (1.0 μM) and the charged single-stranded nonamer fragment (1.0 μM), we observed only a modest difference (2-fold) in the rate of peptide synthesis between the charged fragment (27.6×10^{-9} M min^{-1}) and the charged minihelix^{Ala} (56.7×10^{-9} M min^{-1}) (Figure 3 and Figure 5c). [A rate of 59.0×10^{-9} M min^{-1} was observed for AcAla-tRNA^{Ala} under these same reaction conditions (data not shown).] However, when both the 50S ribosome and the charged fragment are present at low concentrations, the "fragment" is not an efficient substrate (Figure 5a,b). This comparison between the substrates showed that the rate of the peptidyl transfer reaction is nearly independent of the RNA substrate once the substrate is bound.

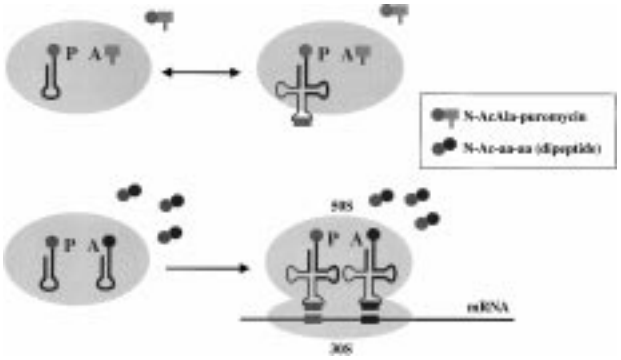

FIGURE 6: (Top) Model system used in this study demonstrating the functional equivalence of the minihelix domain of tRNA and the intact tRNA as ribosome P-site substrates. The A-site substrate is puromycin. The minihelix domain is shown in thick lines, and the anticodon-D-stem−loop domain of intact tRNA is shown with thin lines. (Bottom) Model for the proposed historical development of the present day 70S ribosome from an RNA minihelix−50S ribosome based system for peptidyl transfer reactions. Amino acids and anticodons/codons are represented by filled circles and rectangles, respectively.

DISCUSSION

The tRNA minihelix domain (acceptor stem and TΨC stem−loop) including its 3′-CCA trinucleotide is thought to have arisen early in evolution, possibly in an RNA world that predated the theater of proteins. Its original role may have been as a tag for replication of RNA genomes, and later was captured as a substrate for aminoacylation by ribozymes (*49, 50*). The structures/sequences in minihelices that confer specific aminoacylation constitute an operational RNA code for amino acids that may have predated the genetic code (*14, 51*). Schemes for duplication and recombination of minihelices to give the full tRNA explain the triplets of the genetic code as arising from elements of the operational RNA code (*52*−*55*). The robust peptide synthesis reported here with charged minihelices and 50S ribosomes suggests that this system could be a significant precursor in the development of template-dependent protein synthesis (Figure 6, top panel). If schemes for duplication of minihelices to give tRNAs and the code are relevant, then these duplications may have proceeded in parallel with the addition to the ribosome of the progenitor to the 30S particle. Thus, with the addition of the second domain of tRNA to the minihelix and the emergence of the 30S ribosome, template-dependent protein synthesis was established (Figure 6, lower panel).

Our data show that the minihelix domain is equivalent to the full tRNA as a ribosome P-site substrate (Figure 6, upper

panel) and that, at low RNA and 50S ribosome concentrations, both species are substantially more robust than a charged single-stranded fragment encompassing the 3′-terminal nucleotides of $tRNA^{Ala}$. Because almost the same rate of peptide synthesis is achieved with all three substrates at high concentrations, the deficiency in the single-stranded fragment seems mostly related to a weaker interaction with the 50S ribosome. Possibly the interaction with the ribosome is most optimal with a double-helical segment attached to the four single-stranded nucleotides at the 3′-end. Further experiments are needed to determine whether all 12 base pairs of the minihelix are required, and whether the hairpin loop plays any role. Regardless of these details, the data presented here suggest that the minihelix motif would have a strong selective advantage as a substrate for emerging systems of peptide synthesis (Figure 6).

The tRNA synthetases are divided into two classes, based on the architecture of their active-site-containing domains (*56*−*58*). Regardless of the class to which a synthetase belongs, to a first approximation the enzymes are also made up of two domains (*14*, *42*, *59*−*62*). In addition to the historical, active-site-containing domain, there is a second domain that typically is idiosyncratic to the enzyme. This second domain is thought to have been added later in evolution. In the synthetase−tRNA complex, the active-site-containing domain interacts with the minihelix part of the tRNA, while in most cases the second domain of the synthetase makes contact with the second, anticodon-containing domain of the tRNA. Thus, the ribosome, tRNA, and tRNA synthetases share in common a format where interactions with the catalytic unit (50S ribosome, active-site domain of synthetase, and 3′-acceptor end of tRNA) occur in a domain that is distinct from that which involves the triplets of the genetic code (30S ribosome, second domain of tRNA synthetases, and anticodon-containing domain of tRNA). After the robust system of minihelix-based peptide synthesis demonstrated here was first established, the synthetases could have added their second domain in coordination with the appearance of the progenitor to the 30S ribosome and the second domain of tRNA.

REFERENCES

1. Fox, G. W., and Woese, C. R. (1975) *Nature 256*, 505−507.
2. Noller, H. F. (1984) *Annu. Rev. Biochem. 53*, 119−162.
3. Wool, I. G., Chan, Y. L., and Gluck, A. (1995) *Biochem. Cell Biol. 73*, 933−947.
4. Moore, P. B. (1993) in *The RNA World* (Gesteland, R. F., and Atkins, J. F., Eds.) pp 119−135, Cold Spring Harbor Laboratory Press, Cold Spring Harbor, NY.
5. Traub, P., and Nomura, M. (1968) *Proc. Natl. Acad. Sci. U.S.A. 59*, 777−784.
6. Nomura, M., Traub, P., and Bechmann, H. (1968) *Nature 219*, 793−799.
7. Nomura, M., and Erdmann, V. A. (1970) *Nature 228*, 744−748.
8. Cooperman, B. S., Wooten, T., Romero, D. P., and Traut, R. R. (1995) *Biochem. Cell Biol. 73*, 1087−1094.
9. Weitzmann, C. J., Cunningham, P. R., Nurse, K., and Ofengand, J. (1993) *FASEB J. 7*, 177−180.
10. Monro, R. E. (1969) *Nature 223*, 903−905.
11. Lapointe, J., and Giegé, R. (1991) in *Translation in Eukaryotes* (Trachsel, H., Ed.) pp 35−69, CRC Press, Inc., Boca Raton.
12. Giegé, R., Puglisi, J. D., and Florentz, C. (1993) *Prog. Nucleic Acid Res. Mol. Biol. 45*, 129−206.
13. Francklyn, C., and Schimmel, P. (1989) *Nature 337*, 478−481.
14. Schimmel, P., Giegé, R., Moras, D., and Yokoyama, S. (1993) *Proc. Natl. Acad. Sci. U.S.A. 90*, 8763−8768.
15. Francklyn, C., Shi, J.-P., and Schimmel, P. (1992) *Science 255*, 1121−1125.
16. Nureki, O., Niimi, T., Muto, Y., Kanno, H., Kohno, T., Muramatsu, T., Kawai, G., Miyazawa, T., Giegé, R., Florentz, C., and Yokoyama, S. (1993) in *The Translation Apparatus* (Nierhaus, K. H., Franceschi, F., Subramanian, A. R., Erdmann, V. A., and Wittman-Liebold, B., Eds.) pp 59−66, Plenum Press, New York.
17. Frugier, M., Florentz, C., and Giegé, R. (1994) *EMBO J. 13*, 2218−2226.
18. Hamann, C. S., and Hou, Y.-M. (1995) *Biochemistry 34*, 6527−6532.
19. Saks, M. E., and Sampson, J. R. (1996) *EMBO J. 15*, 2843−2849.
20. Shi, P. Y., Weiner, A. M., and Maizels, N. (1998) *RNA 4*, 276−284.
21. Rudinger, J., Blechschmidt, B., Ribeiro, S., and Sprinzl, M. (1994) *Biochemistry 33*, 5682−5688.
22. Nazarenko, I. A., and Uhlenbeck, O. C. (1995) *Biochemistry 34*, 2545−2552.
23. Rudinger, J., Hillenbrandt, R., Sprinzl, M., and Giegé, R. (1996) *EMBO J. 15*, 650−657.
24. McClain, W. H., Guerrier-Takada, C., and Altman, S. (1987) *Science 238*, 527−530.
25. Noller, H. F. (1998) in *The RNA World* (Gesteland, R. F., Cech, T. R., and Atkins, J. F., Eds.) 2nd ed., pp 197−219, Cold Spring Harbor Laboratory Press, Cold Spring Harbor, NY.
26. Rose, S. J. D., Lowary, P. T., and Uhlenbeck, O. C. (1983) *J. Mol. Biol. 167*, 103−117.
27. Moazed, D., and Noller, H. F. (1986) *Cell 47*, 985−994.
28. Huttenhofer, A., and Noller, H. F. (1992) *Proc. Natl. Acad. Sci. U.S.A. 89*, 7851−7855.
29. Moazed, D., and Noller, H. F. (1991) *Proc. Natl. Acad. Sci. U.S.A. 88*, 3725−3728.
30. Samaha, R. R., Green, R., and Noller, H. F. (1995) *Nature 377*, 309−314.
31. Lieberman, K. R., and Dahlberg, A. E. (1995) *Prog. Nucleic Acid Res. Mol. Biol. 50*, 1−23.
32. Monro, R. E. (1967) *J. Mol. Biol. 26*, 147−151.
33. Monro, R. E., and Marcker, K. A. (1967) *J. Mol. Biol. 25*, 347−350.
34. Monro, R. E., Cerna, J., and Marcker, K. A. (1968) *Proc. Natl. Acad. Sci. U.S.A. 61*, 1042−1049.
35. Ribas de Pouplana, L., and Schimmel, P. (1997) *Biochemistry 36*, 15041−15048.
36. Wincott, F., DiRenzo, A., Shaffer, C., Grimm, S., Tracz, D., Workman, C., Sweedler, D., Gonzalez, C., Scaringe, S., and Usman, N. (1995) *Nucleic Acids Res. 23*, 2677−2684.
37. Moazed, D., and Noller, H. F. (1989) *Cell 57*, 585−597.
38. Haenni, A. L., and Chapeville, F. (1966) *Biochim. Biophys. Acta 114*, 135−148.
39. Nitta, I., Ueda, T., and Watanabe, K. (1998) *RNA 4*, 257−267.
40. Nitta, I., Kamada, Y., Noda, H., Ueda, T., and Watanabe, K. (1998) *Science 281*, 666−669.
41. Shi, J.-P., and Schimmel, P. (1991) *J. Biol. Chem. 266*, 2705−2708.
42. Buechter, D. D., and Schimmel, P. (1993) *Biochemistry 32*, 5267−5272.
43. Green, R., and Noller, H. F. (1996) *RNA 2*, 1011−1021.
44. Khaitovich, P., Tenson, T., Mankin, A. S., and Green, R. (1999) *RNA 5* (in press).
45. Silverstein, E. (1969) *Cold Spring Harb. Symp. Quant. Biol. 34*, 366−368.
46. Donis-Keller, H., Maxam, A. M., and Gilbert, W. (1977) *Nucleic Acids Res. 4*, 2527−2538.
47. Fahnestock, S., Neumann, H., Shashoua, V., and Rich, A. (1970) *Biochemistry 9*, 2477−2483.
48. Odom, O. W., and Hardesty, B. (1992) *J. Biol. Chem. 267*, 19117−19122.

49. Weiner, A. M., and Maizels, N. (1987) *Proc. Natl. Acad. Sci. U.S.A. 84*, 7383−7387.
50. Maizels, N., and Weiner, A. M. (1993) in *The RNA World* (Gesteland, R. F., and Atkins, J. F., Eds.) pp 577−602, Cold Spring Harbor Laboratory, Plainview, NY.
51. Schimmel, P., and Ribas de Pouplana, L. (1995) *Cell 81*, 983−986.
52. Rodin, S., Ohno, S., and Rodin, A. (1993) *Proc. Natl. Acad. Sci. U.S.A. 90*, 4723−4727.
53. Rodin, S., Rodin, A., and Ohno, S. (1996) *Proc. Natl. Acad. Sci. U.S.A. 93*, 4537−4542.
54. Dick, T. P., and Schamel, W. W. A. (1995) *J. Mol. Evol. 41*, 1−9.
55. Moller, W., and Janssen, G. M. C. (1992) *J. Mol. Evol. 34*, 471−477.
56. Webster, T. A., Tsai, H., Kula, M., Mackie, G. A., and Schimmel, P. (1984) *Science 226*, 1315−1317.
57. Eriani, G., Delarue, M., Poch, O., Gangloff, J., and Moras, D. (1990) *Nature 347*, 203−206.
58. Cusack, S., Berthet-Colominas, C., Hartlein, M., Nassar, N., and Leberman, R. (1990) *Nature 347*, 249−255.
59. Moras, D. (1992) *Trends Biochem. Sci. 17*, 159−164.
60. Delarue, M., and Moras, D. (1993) *BioEssays 15*, 675−687.
61. Cusack, S. (1995) *Nat. Struct. Biol. 2*, 824−831.
62. Burbaum, J. J., and Schimmel, P. (1991) *Biochemistry 30*, 319−324.

BI991126F